Environ Sci Pollut Res (2017) 24:28175–28189
https://doi.org/10.1007/s11356-017-0404-5

RESEARCH ARTICLE

Role of sulfate, chloride, and nitrate anions on the degradation of fluoroquinolone antibiotics by photoelectro-Fenton

Paola Villegas-Guzman[1] · **Florian Hofer**[1] · **Javier Silva-Agredo**[1] · **Ricardo A. Torres-Palma**[1]

Received: 25 May 2017 / Accepted: 2 October 2017 / Published online: 10 October 2017

Abstract Taking ciprofloxacin (CIP) as a fluoroquinolone antibiotic model, this work explores the role of common anions (sulfate, nitrate, and chloride) during the application of photoelectro-Fenton (PEF) at natural pH to degrade this type of compound in water. The system was composed of an IrO_2 anode, Ti, or gas diffusion electrode (GDE) as cathode, Fe^{2+}, and UV (254 nm). To determine the implications of these anions, the degradation pathway and efficiency of the PEF sub-processes (UV photolysis, anodic oxidation, and electro-Fenton at natural pH) were studied in the individual presence of the anions. The results highlight that degradation routes and kinetics are strongly dependent on electrolytes. When chloride and nitrate ions were present, indirect electro-chemical oxidation was identified by electro-generated HOCl and nitrogenated oxidative species, respectively. Additionally, direct photolysis and direct oxidation at the anode surface were identified as degradation routes. As a consequence of the different pathways, six primary CIP by-products were identified. Therefore, a scheme was proposed representing the pathways involved in the degradation of CIP when submitted to PEF in water with chloride, nitrate, and sulfate ions, showing the complexity of this process. Promoted by individual and synergistic actions of this process, the PEF system leads to a complete elimination of CIP with total removal of antibiotic activity against *Staphylococcus aureus* and *Escherichia coli*, and significant mineralization. Finally, the role of the anions was tested in seawater containing CIP, in which the positive contributions of the anions were partially suppressed by its OH radical scavenger action. The findings are of interest for the understanding of the degradation of antibiotics via the PEF process in different matrices containing sulfate, nitrate, and chloride ions.

Keywords Water treatment · Advanced oxidation processes · Antimicrobial activity · By-products · Degradation pathways · Complementary processes

Responsible editor: Vítor Pais Vilar

Electronic supplementary material The online version of this article (https://doi.org/10.1007/s11356-017-0404-5) contains supplementary material, which is available to authorized users.

✉ Ricardo A. Torres-Palma
ricardo.torres@udea.edu.co

[1] Grupo de Investigación en Remediación Ambiental y Biocatálisis (GIRAB), Instituto de Química, Facultad de Ciencias Exactas y Naturales, Universidad de Antioquía UdeA, Calle 70 No. 52-21, Medellin, Colombia

Introduction

Advanced oxidation processes (AOPs) have been shown to be highly efficient in the elimination of organic pollutants (Malpass et al. 2007; Klamerth et al. 2013; Villegas-Guzman et al. 2014; Serna-Galvis et al. 2016). This arises from the formation of high oxidative species, mainly the hydroxyl radical (HO•) (E^o = 2.80 V/NHE), which present low selectivity and high reactivity (Brillas et al. 2009; Rubio-Clemente et al. 2014). Due to its efficiency, simplicity, and relatively low cost, the homogeneous Fenton system is probably the most tested AOP. This process is based on the fast production of hydroxyl radicals from the decomposition of hydrogen peroxide by ferrous ions (Eq. 1) (Pignatello et al. 2006). The efficiency of the process is drastically enhanced in the presence of light, due to the regeneration of the ferrous ions and the formation of extra hydroxyl radicals (Eq. 2). Additionally, the interaction of UV-C radiation (e.g., photons of 254 nm, UV_{254}) could contribute to the degradation of the organic pollutants in two ways: the photodecomposition of the hydrogen peroxide to produce

hydroxyl radicals (Eq. 3), and the photodecomposition of organic pollutants (Eq. 4) (Babić et al. 2013; Guo et al. 2013; Sturini et al. 2015; Porras et al. 2016).

$$Fe^{2+} + H_2O_2 \rightarrow Fe^{3+} + OH^- + HO\bullet \quad (1)$$

$$Fe(OH)^{2+} + h\nu \rightarrow Fe^{2+} + HO\bullet \quad (2)$$

$$H_2O_2 + h\nu \rightarrow 2\,HO\bullet \quad (3)$$

$$P + h\nu \rightarrow P_{ox} \quad (4)$$

Despite the benefits of Fenton-based processes, real applications of these are limited because of the complexity of water matrices. It has been recognized that the water matrix has a direct influence on the degradation rates and pathways of the elimination of organic pollutants when AOPs are used (Guzman-Duque et al. 2011; Xiao et al. 2014; Villegas-Guzman et al. 2015). In the case of inorganic anions, inhibitor effects have been reported for the Fenton process, mainly attributed to the HO• scavenger action of some anions (Eqs. 5–7) (Grebel et al. 2010; Guzman-Duque et al. 2011; Devi et al. 2013).

$$Cl^- + HO\bullet \rightarrow HOCl\bullet^- \quad (5)$$

$$SO_4^{2-} + HO\bullet \rightarrow SO_4\bullet^- + OH^- \quad (6)$$

$$NO_3^- + HO\bullet \rightarrow NO_3\bullet + OH^- \quad (7)$$

Additionally, the complexity of the matrix might lead to limitations of the precursors of the Fenton process through simultaneous reactions between these and the matrix. An example of this is the possible interaction of the iron species with some anions to produce iron-ion complexes with low reactivity (Pignatello et al. 2006; Devi et al. 2013). In contrast, electrochemical processes are favored by the presence of inorganic species due to both the decrease of the electric resistance and its possible participation in the formation of extra oxidative species, which are also able to degrade organic pollutants (Comninellis 1994; Martínez-Huitle and Brillas 2009; Aquino et al. 2012). Therefore, the combination of electrochemical systems and the Fenton reaction could be an interesting alternative treatment for complex matrices with a significant concentration of inorganic anions.

The Fenton reaction in which at least one of the precursors is electro-generated is known as the electro-Fenton system (EF). For instance, a continuous electro-generation of hydrogen peroxide can be brought about by the interaction of oxygen and a gas diffusion electrode (GDE) (Brillas et al. 2009). The participation of light radiation in the system is known as photoelectro-Fenton (PEF), a remarkable system in which the production of hydroxyl radicals, and even other reactive species, is highly efficient. Several cathodic materials have been tested for hydrogen peroxide electro-generation, of which GDE has been shown to be highly efficient (Sirés et al. 2014; Bañuelos et al. 2014; Luo et al. 2015). The electro-generation of hydrogen peroxide ($H_2O_{2\ electro\text{-}generated}$) is a multiphase reaction that occurs in the presence of gaseous oxygen, dissolved protons, and electrons (Eq. 8).

$$O_2 + 2H^+ + 2e^- \rightarrow H_2O_{2\ electro\text{–}generated} \quad (8)$$

Depending on the composition of the anode in the PEF system, the electro-oxidation process (EO) can also occur, contributing to the elimination of the pollutants (Espinoza et al. 2016). The efficiency of EO as a treatment process is closely related to the anode material, where hydroxyl radicals, secondary oxidative species, or direct oxidation can promote the oxidation of organic molecules (Aquino Neto and de Andrade 2009; Palma-Goyes et al. 2010; Zhou et al. 2011). At present, boron-doped diamond (BDD) is the preferred anode to degrade organic compounds due to its high production of •OH (Panizza and Martinez-Huitle 2013). However, the cost of the material limits its applicability. Additionally, according to recent investigations, this anode is passivated by the presence of chloride ions, one of the most common anions in water (Guzmán-Duque et al. 2014), reducing its viability of application in many complex water matrices. In contrast, dimensionally stable anodes (DSA) are constituted by lower-cost materials and are not negatively affected by inorganic anions, making their application more feasible (Coria et al. 2016).

Meanwhile, because PEF is an electro-advanced oxidation process, the electrolyte nature also significantly influences the performance of the process. For example, Thiam et al. (2014) evaluated the effect of NaCl, Na_2SO_4, and $NaNO_3$ on the decolorization and TOC removal of a tartrazine dye solution by the PEF/UVA process, and Daneshvar et al. (2008) compared the effect of NaCl, Na_2SO_4, and $NaClO_4$ on the degradation of an orange II dye solution by the EF process. Both investigations found that the presence of ions such as chloride can promote the generation of additional oxidative species, which participate in the degradation of organic pollutants. On the other hand, the possible formation of chloro- or sulfato-iron complexes decreases the concentration of free ferrous ions and consequently inhibits the Fenton reaction (Daneshvar et al. 2008). As previously indicated, anions can also act as OH radical scavengers. Nonetheless, the above-mentioned works and many others have highlighted the good performance of the PEF process in the degradation of organic pollutants in water. However, most of these works have evaluated synthetic water containing only one of the ions, employed as a supporting electrolyte. Therefore, evaluation in more realistic conditions, i.e., in water containing a mix of several ions, is still limited.

With regard to the nature of pollutants, special attention has been addressed to emergent contaminants (ECs) such as pharmaceutical products (Pérez et al. 2017). Among these, antibiotics are key targets for degradation given the risks they present

to humans and the environment, in particular with respect to bacteria resistance (Gatica and Cytryn 2013). This is the case with the antibiotic ciprofloxacin (CIP), the most highly consumed fluoroquinolone antibiotic in Europe (Xu et al. 2007; De Bel et al. 2009), due to its broad-spectrum action, which has been found in several water matrices. In the present work, the role of inorganic ions commonly found in several types of water matrices during application of PEF at natural pH was investigated, taking ciprofloxacin (CIP) as a fluoroquinolone antibiotic model. A previous investigation used the PEF system for the degradation of CIP in urine with encouraging results (Antonin et al. 2015). In the study, the antibiotic was totally eliminated and high levels of mineralization were reached. However, the participation of different ions was not discussed. Additionally, the process was carried out at pH 3, reducing the possibility of practical applications of the technology.

Therefore, this investigation evaluates for the first time the role of common inorganic ions (chloride, sulfate, and nitrate) during the application of PEF as an alternative water treatment. The efficiency of PEF in degrading fluoroquinolones with no pH modification was investigated, in terms of CIP elimination, mineralization level, and antibiotic activity elimination. For better understanding of the PEF system, the efficiency of the sub-processes involved (UV_{254}, EO, and EF) was individually evaluated. Thus, the degradation pathways and the nature of CIP transformations during the PEF system according to the anions in solution were determined. Finally, the effect of the simultaneous presence of the anions in the efficiency of the PEF process was investigated by determining the evolution of the pollutant, antibiotic activity, and mineralization level in simulated seawater in the presence of the three anions.

Methodology

Reagents

CIP was provided by Laproff (65% purity). Acetonitrile, ammonium metavanadate, boric acid, iron sulfate, methanol, potassium hydrogen phtalate, ammonium heptamolybdate, sodium chloride, sodium sulfate, sulfuric acid, oxalic acid, potato dextrose agar, and nutritive agar were provided by Merck. Calcium chloride, magnesium chloride, potassium bromide, potassium chloride, potassium iodide, sodium bicarbonate, sodium fluoride, and strontium chloride were purchased from Carlo Erba.

Electro-chemical cell

The experiments were carried out in a 250-mL, one-compartment, glass electro-chemical cell equipped with an external lamp. Irradiation was achieved using an 8-W lamp (OSRAM Germicidal Puritec) with maximum emission at 254 nm. The liquid was recirculated at 34 mL min^{-1} using an ISMATEC VP Antrieb pump. The electro-chemical cell was composed of a 4.9-cm^2 gas diffusion electrode (GDE) made of a ELATTMLT-1400 membrane provided by NuVant Systems Inc. and a 4-cm^2 dimensionally stable anode (DSA) made of iridium oxide deposited on titanium (Ti/IrO_2). Air was pumped through the GDE cathode at 840 mL min^{-1} using an AC-1500 Resun Air Pump. The electro-chemical cell was placed on a magnetic stirrer to guarantee the complete solution homogenization during the experiments. In order to select the applied current, provided by a Thurlby Thandar PL330 power supply, it was taken into account that higher current densities increase the formation of oxidative species (Palma-Goyes et al. 2010; Guzmán-Duque et al. 2014) and that current densities over 30 mA cm^{-2} might produce harmful inorganic chlorine species (e.g., ClO_3^- or ClO_4^-) (Sánchez-Carretero et al. 2011; Lacasa et al. 2013). Therefore, in order to preclude the formation of such species, and to limit the cathodic reduction of the oxidative HOCl specie (Rudolf et al. 1995), a relatively low current of 20 mA (~ 5 mA cm^{-2}) was chosen. To test the sole Ti/IrO_2 anode action, experiments with Ti cathode in the absence of light were also performed. In order to remove iron deposits on the cathode, the GDE membrane was washed for 30 min in oxalic acid solution (10% *w*/*w*) prior to each experiment. For all the experiments, the solutions tested were prepared by mixing 50 mM of the supporting electrolyte (NaCl, Na_2SO_4, or $NaNO_3$) with 0.1 mM of CIP. Finally, 0.09 mM of Fe^{2+} was added to the reaction vessel. All the experiments were performed at least twice.

Apparatus and analytic methods

The concentration of ciprofloxacin was determined using a UHPLC Thermo Scientific Dionex UltiMate 3000 equipped with a Thermo Acclaim C-18 column (particle size 5 μm, dimensions 100 × 4.6 mm) and a DAD detector. A mix of phosphate buffer (0.02 M, pH 3)/acetonitrile, 70/30 (% vol.), was used as mobile phase at a flow rate of 0.8 mL min^{-1}. The mineralization extent was determined by total organic carbon (TOC) using a Shimadzu total organic carbon analyzer (TOC-5000A). The calibration curve was obtained with a standard solution of potassium hydrogen phthalate. Two different spectrophotometric procedures were used to quantify the amount of oxidants in solution: the iodometric method for the determination of all oxidants (Villegas-Guzman et al. 2014) and the metavanadate method, which is specifically for hydrogen peroxide quantification (Nogueira et al. 2005). In both cases, a Jenway 6320D spectrophotometer was used. The antibiotic activity (AA) was measured using *Escherichia coli* (Gram-negative) and *Staphylococcus aureus* (Gram-positive) as tested bacteria. The petri dishes were prepared with a base layer of potato dextrose agar (~ 5 mL), over which poured nutritive agar (~ 10 mL) was poured containing 10 μL of bacteria

solution (0.6 units of absorbance at 560 nm). Twenty microliters of sample was then added to the petri dish and, after 24 h, the inhibiting halo was measured.

Results and discussion

Effect of common anions during the application of PEF

The water matrix composition can promote inhibiting reactions or alternative degradation pathways during the treatment of organic pollutants, which can affect the efficiency of the applied process in terms of pollutant elimination, mineralization (TOC removal) and, for antibiotics such as CIP, antibiotic activity (AA) elimination. Moreover, the PEF system tested can be considered as a synergistic combination of several subprocesses (photolysis (UV), electro-oxidation (EO), and electro-Fenton (EF)), the efficiency of which can be improved or diminished by the inorganic anions. Therefore, the investigation of the influence of common anions on PEF efficiency in degrading organic pollutants becomes necessary. For this purpose, the effect of chloride, sulfate, and nitrate in the PEF system and its sub-processes EO, EF, and UV is individually evaluated in this section.

Effect of sulfate ions

In order to elucidate the role of sulfate ions in the PEF system and its sub-processes, a set of experiments with the sole presence of sodium sulfate as supporting electrolyte was carried out. CIP elimination and TOC removal by PEF, UV_{254}, EF, and EO are shown in Fig. 1a. As can be seen, with the light action alone (UV_{254}), ~ 95% of CIP was eliminated in 3 h (reaction rate 1.62×10^{-3} mM min^{-1}). As has been previously demonstrated (Porras et al. 2016), the photoexcitation of CIP generates the triplet excited state $^3CIP^*$ (Eqs. 9–10). This state can produce photoproducts (Eq. 11), or react with molecular oxygen to form singlet oxygen (Eq. 12) or superoxide anion (Eq. 13), which are also able to degrade CIP. However, no mineralization is reached (Fig. 1a), indicating that the by-products generated are stable during the light action.

$$CIP + h\nu \rightarrow {}^1CIP^* \quad (9)$$

$${}^1CIP^* \rightarrow {}^3CIP^* \quad (10)$$

$${}^3CIP^* \rightarrow photoproducts \quad (11)$$

$${}^3CIP^* + O_2 \rightarrow CIP + {}^1O_2 \quad (12)$$

$${}^3CIP^* + O_2 \rightarrow CIP^+ + O_2\bullet^- \quad (13)$$

Regarding EO action, it can be observed that after 180 min, only ~ 15% of CIP was eliminated, with an initial degradation rate of 0.31×10^{-3} mM min^{-1}, while the TOC removal was negligible. To better understand these results, the formation and accumulation of oxidative species was also measured during the EO system process (Fig. 1b). Neither hydrogen peroxide nor any oxidative species were observed in the oxidant accumulation measured. This indicates that, under work conditions, the cathode used for this experiment (Ti) does not electro-generate oxidants, and the electrolyte does not induce any oxidative specie. Hence, the finding suggests that CIP oxidation using EO in the presence of sulfate anion can be attributed to its direct oxidation on the anode surface. Although the anode used (Ti/IrO_2) has a low over-potential for oxygen evolution, direct oxidation of organic molecules on its surface has been reported [23–24]. Direct electro-chemical oxidation can take place in two ways: by electron transfer from the pollutant to the Ti/IrO_2 surface (Eq. 14), or by the oxidation of the IrO_3 sites at the anode (Eq. 15), which arises from the water discharge on the IrO_2 surface (Eqs. 16–17). In order to elucidate the direct electro-chemical degradation route involved, cyclic voltammetry tests were carried out (Supporting material, SM1). As can be seen, no signal attributed to CIP oxidation is observed. So, direct electron transfer at the IrO_2 surface is not plausible. Therefore, direct CIP degradation can be associated to the oxidation at IrO_3 sites formed prior to the water discharge (Eqs. 16–17). Direct oxidation of another antibiotic, oxacillin, by IrO_3 sites was also found by Giraldo et al. (2015). This degradation route is highly limited by diffusional effects, leading to a slow initial degradation rate. Consequently, low pollutant degradation (15%) and negligible mineralization was obtained by EO action in the presence of sulfate ions.

$$CIP \rightarrow CIP_{ox} + e^- \quad (14)$$

$$IrO_3 + CIP \rightarrow CIP'_{ox} \quad (15)$$

$$IrO_2 + H_2O \rightarrow H^+ + IrO_2(HO\bullet) + e^- \quad (16)$$

$$IrO_2(HO\bullet) \rightarrow IrO_3 + H^+ + e^- \quad (17)$$

In contrast, CIP was totally and rapidly eliminated by both EF and PEF systems, with quite similar degradation rates (5.82×10^{-3} and 5.94×10^{-3} mM min^{-1}, respectively). In spite of that, the absence of mineralization during the EF process was again observed (Fig. 1a). In contrast, ~ 60% of the initial TOC was removed by the PEF action after 120 min. The high mineralization efficiency of the PEF system can therefore be attributed to the synergistic participation of the UV_{254} light.

To better explain the results observed, the accumulation of oxidants, specifically H_2O_2, was determined for each Fenton-based process (Fig. 1b). During the application of both processes, the H_2O_2 formation is evident. A control experiment with only H_2O_2 showed no elimination of CIP (data not shown). Thus, under work conditions, H_2O_2 is not directly involved in CIP transformation. The high stability of CIP against this oxidative agent was recently reported (Villegas-

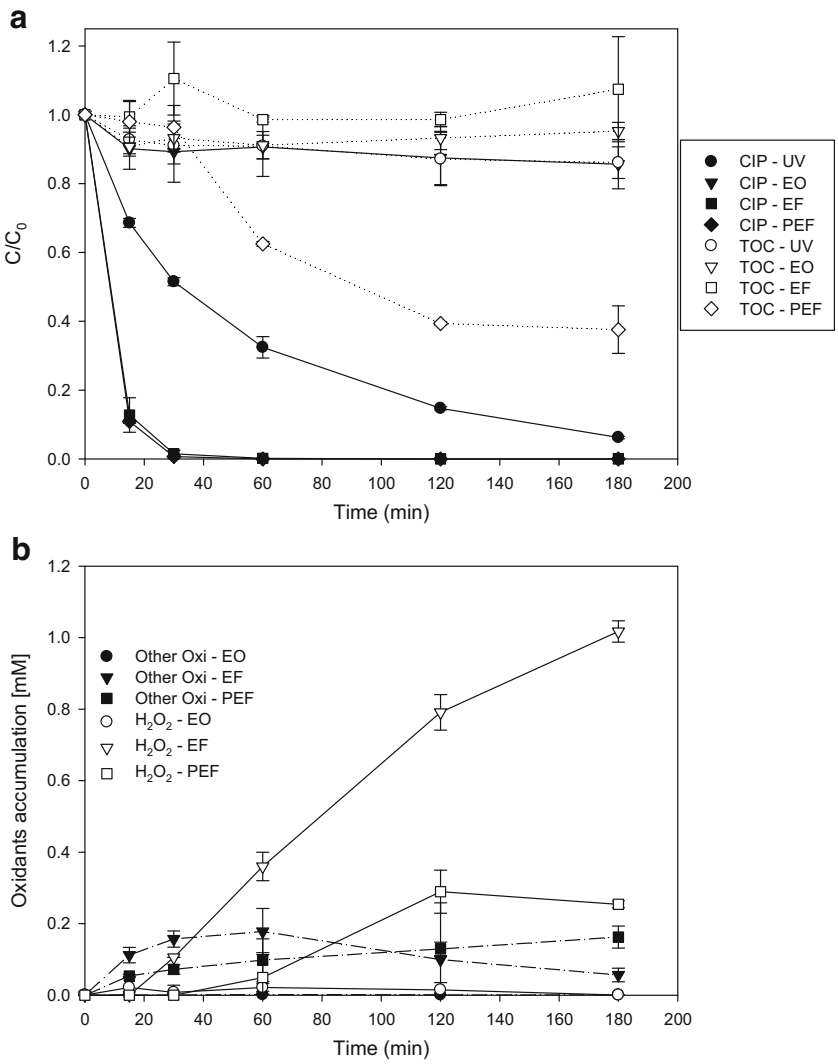

Fig. 1 **a** CIP and TOC evolution in the presence of sulfate as supporting electrolyte when submitted to UV, EO, EF, and PEF. **b** Oxidant accumulation during CIP degradation in the presence of sulfate as supporting electrolyte. [CIP] = 0.1 mM; $[Fe^{2+}]$ = 0.09 mM; i = 20 mA; air flow = 840 mL min^{-1}; reactor flow = 34 mL min^{-1}

Guzman et al. 2017). In turn, H_2O_2 is efficiently converted into HO• radicals through the Fenton reaction. This explains the faster initial degradation rates of the Fenton-based processes compared to the EO and UV action. Interestingly, the H_2O_2 accumulation during the PEF process was significantly less than in EF (Fig. 1b). This could be associated with (i) the photodecomposition of hydrogen peroxide during the PEF process and (ii) the increased Fenton reaction (Eq. 1), due to the light reconversion of Fe^{3+} in Fe^{2+} (Eq. 2). Both phenomena produce extra hydroxyl radicals, which is manifested in a relatively high mineralization extent (60% of TOC removal in 2 h during the PEF system).

Moreover, a small accumulation of other oxidants (Other-Oxi) can be observed in both the EF and PEF systems. This is probably due to the recombination of sulfate radicals (coming from sulfate and hydroxyl radical reaction, Eq. 6) to produce persulfate ions (Eq. 18). Sulfate radical and persulfate ions can also participate in the degradation of CIP and the generated by-products, albeit to a small extent (Serna-Galvis et al. 2017a).

$$2SO_4^{\bullet -} \rightarrow S_2O_8^{2-} \quad (18)$$

Effect of chloride ions

To date, chloride anions present in several types of water have been shown to inhibit the degradation of organic pollutants by Fenton process (Pignatello et al. 2006). On the contrary, the electro-oxidation of organic compounds with Ti/IrO_2 anodes is highly efficient in the presence of Cl^- due to the possible formation of chlorinated oxidative species (Torres et al. 2003; Aquino Neto and de Andrade 2009; Guzmán-Duque et al. 2014). Therefore, the evaluation of the impact of this anion during the PEF process, as well as in its sub-processes, is of interest. The results in Fig. 2a again indicated that, to some extent, UV radiation alone is able to promote CIP degradation with an initial rate (1.16×10^{-3} mM min^{-1}) quite similar to that observed with sulfate (1.62×10^{-3} mM min^{-1}). In addition, again as in the case of sulfate, no difference in the CIP

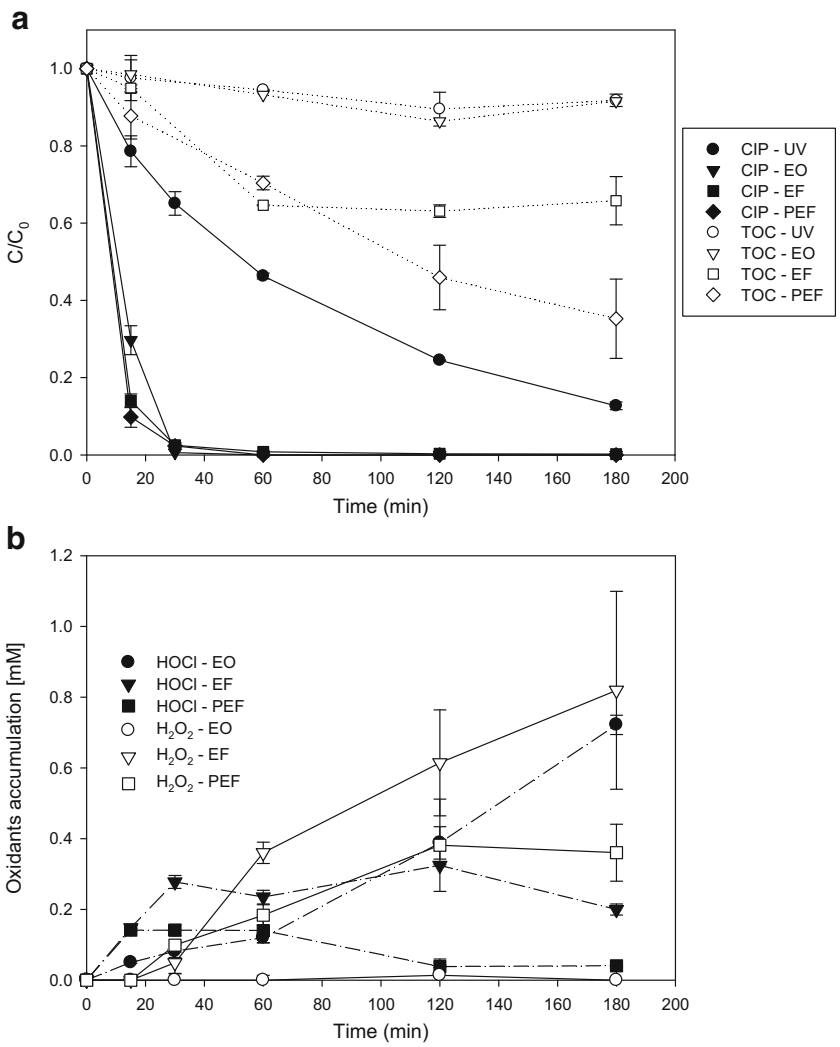

Fig. 2 **a** CIP and TOC evolution in the presence of chlorine as supporting electrolyte when submitted to UV, EO, EF, and PEF. **b** Oxidant accumulation during CIP degradation in the presence of chlorine as supporting electrolyte. [CIP] = 0.1 mM; $[Fe^{2+}]$ = 0.09 mM; i = 20 mA; air flow = 840 mL min^{-1}; reactor flow = 34 mL min^{-1}

elimination profile between PEF and EF systems was observed (initial degradation rates of 6.02×10^{-3} and 5.73×10^{-3} mM min^{-1}, respectively).

Comparing the first 15 min of treatment of all the tested systems in chloride media, CIP elimination was faster in the Fenton-based processes (PEF and EF) than in EO (3.31×10^{-3} mM min^{-1}). However, after 30 min in the presence of chloride, no significant differences among the EO and the two Fenton-based processes were observed, contrary to what was observed using sulfate as electrolyte. In fact, in this time, more than 95% of CIP was eliminated in the three systems. The relative improvement of EO in the presence of chloride suggests the involvement of chlorinated oxidative species in CIP degradation (Torres et al. 2003; Aquino Neto and de Andrade 2009; Guzmán-Duque et al. 2014). The high efficiency of the electro-generated chlorinated oxidative species to degrade fluoroquinolones and other antibiotics, using the same anode, was recently reported (Serna-Galvis et al. 2017a; Serna-Galvis et al. 2017b). Interestingly, the positive effect of chloride ions in the electro-chemical oxidation of organic pollutants is limited neither to antibiotics nor to Ti/IrO_2 anodes. In fact, in the presence of chloride ions, the EO of acid orange 7 with BDD was enhanced (Carvalho et al. 2007), and oxidation of tartrazine dye was improved in both BDD and Pt electrodes (Thiam et al. 2014).

Meanwhile, TOC removal during the EF process with chloride (30% mineralization in 180 min) was drastically better than the removal rate observed in the presence of sulfate (0% mineralization in 180 min). The significant mineralization observed also suggests the participation of several oxidative species, which transform not only CIP but also some of its generated by-products in CO_2, water, and inorganic ions.

On the other hand, neither EO nor UV action achieved significant mineralization (TOC removal). Meanwhile, contrary to what was observed for CIP elimination, differences in the mineralization extent between PEF and EF were significant. During the EF process, only 30% of TOC was removed after 60 min, and further treatment times did not change the mineralization extent. In contrast, during PEF the TOC

removal increased during the treatment and reached almost 70% after 180 min.

All the findings from previous works suggest that the sub-processes involve additional or alternative degradation pathways with a possible participation of chlorinated oxidative species that have an influence on both the degradation and mineralization of CIP. Therefore, the accumulation of oxidants was determined for each process in terms of H_2O_2 and chlorinated oxidative species (Fig. 2b). During EO, no hydrogen peroxide was accumulated, as was expected given the cathode used for this experiment (Ti). On the contrary, accumulation of chlorinated oxidative species was evident during EO action. Based on the chlorinated species equilibrium (Eqs. 19–21) and the change in pH during the experiment (from 5.1 to 4.0), the main oxidative specie during the EO process was hypochlorous acid (HOCl). Therefore, the results of CIP and TOC evolution (Fig. 2a) during the EO test suggest that HOCl can easily eliminate CIP (100% removal in 30 min). However, since no mineralization is reached after the treatment, CIP by-products can be considered recalcitrant to the action of this oxidant.

$$2Cl^- \rightarrow Cl_2 + 2e^- \quad (19)$$

$$Cl_2 + H_2O \leftrightarrow HOCl + H^+ + Cl^- \; pKa = 3.0–7.0 \quad (20)$$

$$HOCl \leftrightarrow H^+ + OCl^- \; pKa = 7.6 \quad (21)$$

On the other hand, during EF and PEF processes, both chlorinated oxidants and H_2O_2 were accumulated, suggesting the participation of both HOCl and HO• during CIP degradation by these processes. This explains the faster initial degradation rates of the Fenton-based processes compared to the EO action. Additionally, the significant participation of HOCl in CIP degradation during EF and PEF processes increases the hydroxyl radicals available to attack CIP by-products, and consequently mineralization is promoted.

It must be mentioned that no accumulation of hydrogen peroxide was observed during the first 15 min in both EF and PEF treatments. On the contrary, in both cases, HOCl was accumulated from the beginning of the experiments. The absence of H_2O_2 accumulation at the first stage of the processes can be attributed to the following facts: (i) the fast decomposition of H_2O_2 by the Fenton reaction (Eq. 1); (ii) the non-recombination of hydroxyl radicals to produce H_2O_2 (Eq. 22), which suggests that the HO• radicals produced are completely consumed by CIP molecules or Cl^- ions (Eq. 6). (iii) The reaction between hydrogen peroxide and hypochlorous acid (Eq. 23) once H_2O_2 concentration in solution is observable (Fig. 2b); this is in line with the lower accumulation of HOCl. The practically zero accumulation of HOCl during PEF can be also explained by its decomposition by light action, which produces additional HO• (Eq. 24) (Feng et al. 2007).

$$HO\bullet + HO\bullet \rightarrow H_2O_2 \quad (22)$$

$$HOCl + H_2O_2 \rightarrow H_2O + O_2 + H^+ + Cl^- \quad (23)$$

$$HOCl + h\nu \rightarrow HO\bullet + Cl\bullet \quad (24)$$

On the other hand, it is also useful to discuss the significant differences between the EF and PEF processes with respect to H_2O_2 accumulation once the first 15 min of treatments elapsed. During the EF process, a continuous accumulation of H_2O_2 was observed, probably associated to the limitation of the Fenton reaction (Eq. 1) once most of the Fe^{2+} is transformed into Fe^{3+}. In turn, during the PEF process, the accumulation of hydrogen peroxide showed a plateau, indicating an equilibrium between its formation and consumption. In the PEF system, the H_2O_2 consumption is also related to the fast regeneration of Fe^{2+} by UV action (Eq. 2) which favors the Fenton reaction (Eq. 1). Furthermore, UV radiation can also promote the photodecomposition of H_2O_2 (Eq. 3). Both light effects lead to the prevention of H_2O_2 accumulation and the formation of extra hydroxyl radicals that could be consumed by the pollutant and its by-products.

All the results from previous works suggest that during PEF treatment of waters containing chloride ions, HClO formed at the anode surface strongly contributes to CIP removal. However, the mineralization achieved can be attributed in practice to the action of HO•, which contrary to HClO is able to transform the pollutant into CO_2, water, and inorganic ions. In spite of that, HOCl seems to play an important role in CIP mineralization, providing additional HO• in solution (Eq. 24).

Effect of nitrate ions

Interestingly, in the presence of nitrate as supporting electrolyte, the EO process reached total elimination of CIP after 60 min of treatment (Fig. 3a), with an initial degradation rate of 2.8×10^{-3} mM min^{-1}. This is only ~ 0.5 times lower than the Fenton-based processes (5.82×10^{-3} mM min^{-1} for EF and 6.21×10^{-3} mM min^{-1} for PEF). Interestingly, in the EO system, the CIP degradation rate observed in the presence of nitrate ions is just a little lower than that observed in the presence of chloride. This suggests that nitrate ions in solution also promote the generation of oxidative species.

Despite this, no significant mineralization was observed during the EF and EO processes in nitrate media. Additionally, in the case of the PEF system, TOC removal in the presence of nitrate was significantly slower compared with the experiments performed in the presence of chloride, but more efficient than those using sulfate. Again, to better understand the above results, the accumulation of oxidants was determined for each process (Fig. 3b). A high accumulation of other oxidants can be observed for

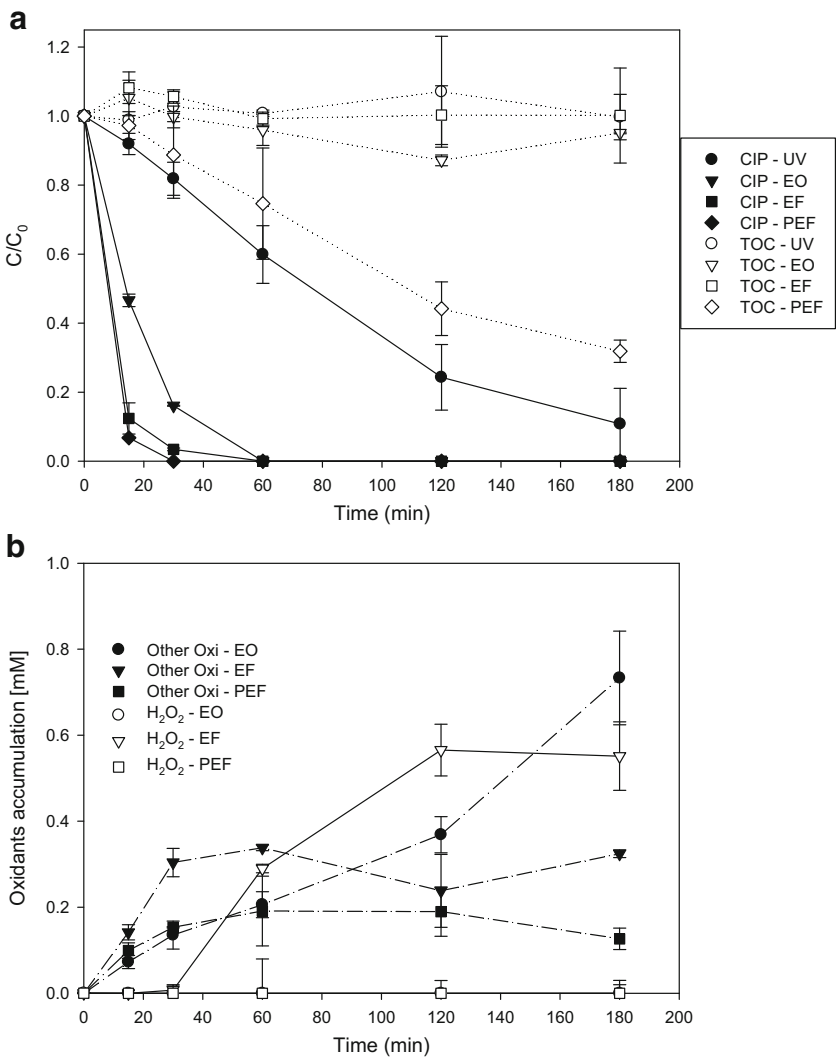

Fig. 3 **a** CIP and TOC evolution in the presence of nitrate as supporting electrolyte when submitted to UV, EO, EF, and PEF. **b** Oxidant accumulation during CIP degradation in the presence of nitrate as supporting electrolyte. [CIP] = 0.1 mM; $[Fe^{2+}]$ = 0.09 mM; i = 20 mA; air flow = 840 mL min^{-1}; reactor flow = 34 mL min^{-1}

the EO system, confirming the formation of oxidative species upon electrolysis of nitrate ions. Considering the high oxidation state of the nitrate ion, its oxidation at the anode is not plausible. Therefore, the oxidants observed could come from the reduction of the anion at the cathode (Ti for EO experiments). Previous investigations have proved that the cathodic reduction of nitrate anions into ammonia is possible through electron transfer with several transition metals in both acidic and alkaline media (Bouzek et al. 2001; Dima et al. 2003; Lacasa et al. 2011, 2012; Liang et al. 2016; Couto et al. 2016). During the reduction process, intermediate products such as nitric oxide (NO, E^o = 1.59 V) or nitrous oxide (N_2O, E^o = 1.77 V) can be generated (Eqs. 25–27). These have similar oxidative powers to HClO (E^o = 1.63 V). Moreover, carbon-based cathodes have also been efficiently tested for the electro-reduction of nitrate ions (Hu et al. 2015). Therefore, during PEF, CIP degradation treatment via nitrogen-based oxidants is a route that can reasonably explain the superior efficiency for CIP and TOC removal for the experiments in the presence of nitrate compared with the results observed in the presence of sulfate. Interestingly, the pH showed a higher decrease (from 4.8 to 3.1) compared with the systems that used sulfate or chloride (from 5.1 to 4.0). This could be also attributed to the cathodic reduction of the nitrate ion, which limits the OH^- formation from water electrolysis at the GDE cathode.

$$NO_3^- + 2H^+ + 2e^- \rightarrow NO_2^- + H_2O \quad (25)$$

$$NO_2^- + 2H^+ + e^- \rightarrow NO + H_2O \quad (26)$$

$$2NO + 2H^+ + 2e^- \rightarrow N_2O + H_2O \quad (27)$$

Regarding the accumulation of oxidants during the Fenton-based processes in the presence of nitrate ions, two effects can be observed. First is the absence of hydrogen peroxide during the first 30 min of both treatments. Second is the significantly lower accumulation of H_2O_2 compared to the experiments in the presence of the other two anions (chlorine and sulfate). In fact, during the PEF test, no hydrogen peroxide was accumulated at all. All these findings support the hypothesis of nitrate

reduction at the cathode that, in the case of the PEF system, limits its capacity to electro-generate H_2O_2. The reduction in H_2O_2 formation explains the lower mineralization observed for the Fenton-based processes in the presence of nitrate compared with the corresponding experiments in the presence of chloride ions.

Overview of CIP degradation pathways by PEF process in water containing sulfate, chloride, and nitrate anions

Currently, real water contaminated with fluoroquinolone antibiotics, such as domestic and industrial wastewater, and seawater, contains a mix of several anions, the most commonly present ions being sulfate, nitrate, and chloride. Therefore, from the findings in "Effect of sulfate ions," "Effect of chloride ions," and "Effect of nitrate ions" sections, it is possible to argue that CIP degradation by PEF in real water containing these anions can involve different pathways where several sub-processes and oxidative species participate in the oxidation of the pollutant (Table 1). Therefore, the results indicate that the OH radical is not the only species responsible for the oxidation. In fact, direct oxidation via IrO_3 was identified, albeit to a relatively small extent. This seems to occur independently of the matrix conditions. Additionally, photolysis and indirect oxidation, depending on the type of anions in solution, can also take place. Hence, CIP degradation can be carried out by HOCl and nitrogen-based oxidants (N_{oxi}) generated from chloride and nitrate ions, respectively.

A schematic figure can be proposed in order to explain the complexity of the PEF steps involved in CIP degradation in matrices containing the tested anions (Fig. 4). As seen, in route 1 (R1) the electro-generation of H_2O_2 by GDE action in the presence of dissolved Fe^{2+} promotes a homogeneous Fenton reaction (Eq. 1), producing HO• radicals that oxidize CIP molecules. Additionally, the GDE cathode can reduce NO_3^-, producing nitrogenated-based oxidants able to contribute to CIP degradation (R2). On the other hand, at the anode, direct CIP anodic oxidation takes place (R3). The DSA anode also promotes the electro-oxidation of chloride to HOCl, which contributes to CIP degradation (R4). Furthermore, in the bulk of the solution, other reactions take place in addition to the Fenton reaction. These are HO• recombination (Eq. 11),

Table 1 CIP degradation pathways under EO, EF, and PEF action using chloride, nitrate, and sulfate as supporting electrolyte

System	EO	EF	PEF
Cl^-	HClO; IrO_3	HO•; HClO; IrO_3	HO•; HClO; IrO_3; hν
NO_3^-	N_{oxi}; IrO_3	HO•; N_{oxi}; IrO_3	HO•; N_{oxi}; IrO_3; hν
SO_4^{2-}	IrO_3	HO•; IrO_3	HO•; IrO_3; hν

[CIP] = 0.1 mM; [Fe^{2+}] = 0.09 mM; i = 20 mA; air flow = 840 mL min^{-1}; reactor flow = 34 mL min^{-1}

the decomposition of H_2O_2 by HOCl (Eq. 12), and the HO• scavenger action of chloride (Eq. 6), sulfate (Eq. 7), and nitrate ions (Eq. 8). Finally, several photochemical reactions are promoted, where both the direct photolysis of CIP (R5) (Eq. 4) and the extra HO• produced from the photolytic action on the iron aquo-complex (Eq. 2), hypochlorous acid (Eq. 24), and hydrogen peroxide (Eq. 3) contribute to CIP elimination.

Seawater is an interesting example of a complex matrix containing sulfate, nitrate, and chloride ions (Table 2), where all of the above-mentioned degradation pathways can contribute to CIP degradation. Figure 5a compares the evolution of CIP when submitted to PEF in two different matrices spiked with the pollutant: distilled water containing chloride ions (DW) and seawater (SW). Due to its higher ion concentration, as well as the higher variety and extent of oxidative species and degradation pathways, one can expect higher CIP elimination in SW. However, CIP removal was almost equal in both types of water. In fact, after 10 min of treatment, 100% of CIP was eliminated in SW and ~ 90% in DW. The results demonstrate that the positive action of the anions can be partially counteracted by their HO• scavenger properties (Eqs. 5–7). The possible interaction of iron with some anions to produce iron-ion complexes with low reactivity (Pignatello et al. 2006; Devi et al. 2013) can also negatively affect the process in SW.

To better interpret the results, TOC was also measured (Fig. 5a). The results show that in DW ~ 70% mineralization was reached after 180 min; at the same time, only ~ 20% of TOC was removed in SW. The low mineralization achievement in SW is consistent with the HO• scavenger properties of the anions. In addition, the extra oxidants produced in SW, mainly coming from the chloride and nitrate ions, are able to transform the initial pollutant but not its degradation by-products.

To further investigate this, the formation and accumulation of oxidants in the course of the process were evaluated (Fig. 5b). As expected, the results showed accumulation of both H_2O_2 and other oxidative species in the two types of water tested. Regarding oxidants other than hydrogen peroxide, no significant differences were seen during the process. However, large differences were observed in the hydrogen peroxide accumulation, which after 180 min was four times higher in DW (~ 0.4 mM) than in SW (0.1 mM). These results are in line with the OH radical scavenger effect of the anions in SW. The lower accumulation of hydrogen peroxide in SW is also due in part to its reaction with HOCl. On the other hand, it is noteworthy that in seawater, the initial pH decreased to ~ 3.2 within the first 60 min of treatment. As previously explained, this could be attributed to water discharge at the anode, the cathodic reduction of nitrate ions, and the possible formation of carboxylic acids prior to mineralization.

Finally, in spite of the strong OH radical scavenger properties of the matrix and several detrimental reactions among the oxidative species, PEF constitutes a very robust system able to efficiently eliminate CIP in a relatively short period

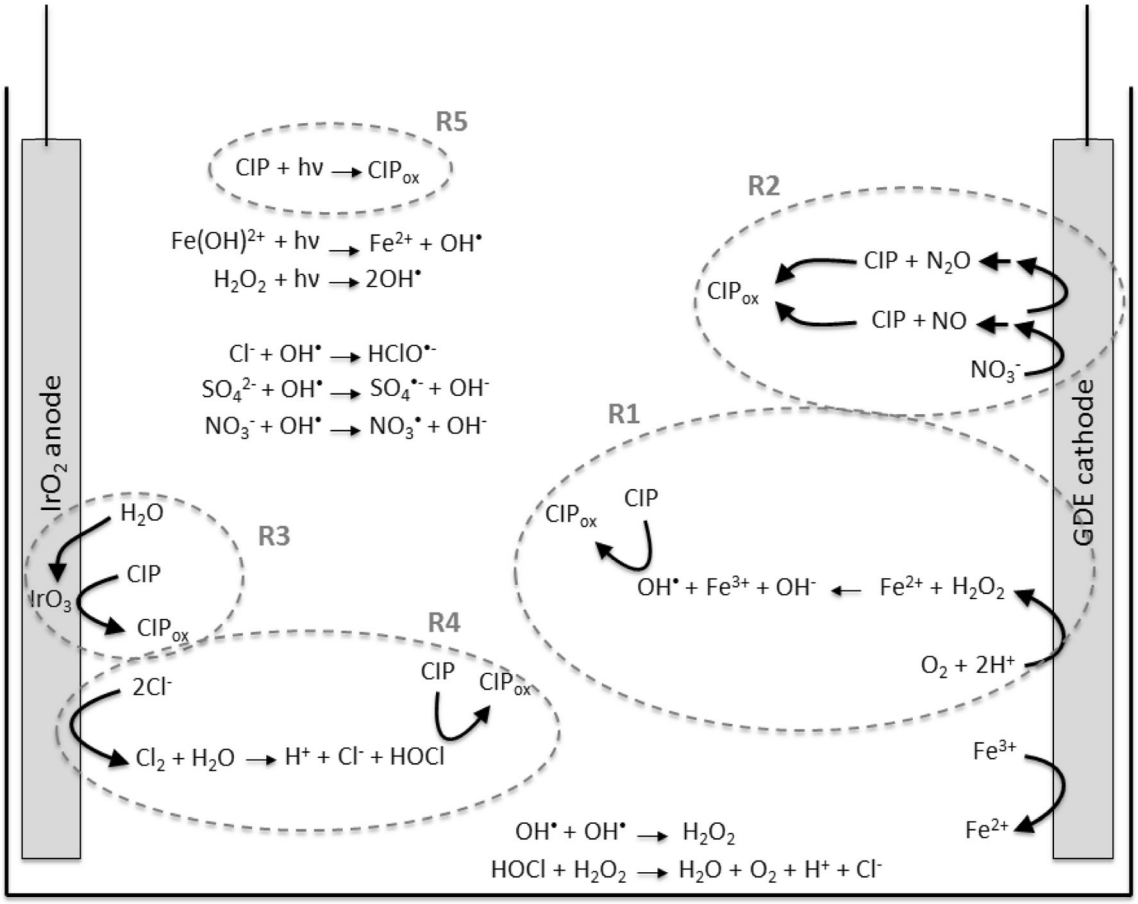

Fig. 4 Schematic representation of initial CIP degradation by PEF process in complex waters with chloride, nitrate, and sulfate ions

of time. However, unlike the pollutant removal efficiency, the complete mineralization extent could be seriously affected. Therefore, and considering the risk of antimicrobial resistance spread by the CIP by-products, the evaluation of the antimicrobial activity of treated CIP solutions and the identification of organic by-products become crucial. This will be addressed in the next section.

Identification of the primary organic by-products and evaluation of the antimicrobial activity of CIP solutions treated with the PEF system

The participation of several pathways during CIP degradation by the PEF process in matrices containing sulfate, nitrate, and chloride ions could be directly involved in the nature of the organic by-products. Therefore, in order to identify the by-products coming from UV action, as well as from the attack of HOCl and HO• radicals during CIP degradation by the PEF treatment, the antibiotic was treated by UV (15 min), EO in the presence of chloride ions (60 min), and EF with nitrate ions (30 min). For each experiment, HPLC/MS analyses were carried out and the UV spectrum of each by-product was performed. Based on the HPLC/MS and the UV spectra analyses for the UV_{254} system (Supporting material, SM2), EF system (Supporting material, SM3) and EO system (Supporting material, SM4), six primary degradation by-products were found (P1, P2, P3, P4, P5, and P6). Figure 6 shows the proposed structures and the sub-processes (UV, EO, and EF) where these compounds were detected. The by-products can be identified as follows: P1, 1-cyclopropyl-6-hydroxy-4-oxo-7-(piperazin-1-yl)-1,4-dihydroquinoline-3-carboxylic acid; P2, 7-[(2-aminoethyl)amino]-1-cyclopropyl-4-oxo-1,4-dihydroquinoline-3-carboxylic acid; P3, 7-[(2-aminoethyl)(formyl)amino]-1-cyclopropyl-6-fluoro-4-oxo-1,4-dihydroquinoline-3-carboxylic acid; P4, 1-cyclopropyl-6-fluoro-7-[(hydroxymethyl)[2-((hydroxymethyl)amino)ethyl]amino]-oxo-1,4-dihydroquinoline-3-carboxylic acid; P5,

Table 2 Tested water characterization

Analysis	TOC_0 [mg C L^{-1}]	Cl^{-1} [mg L^{-1}]	SO_4^{2-} [mg L^{-1}]	NO_3^- [mg L^{-1}]
DW	< 20	772	< 0.2	< 0.2
SW	< 20	19,834	2766	0.512

DW distilled water, *SW* seawater

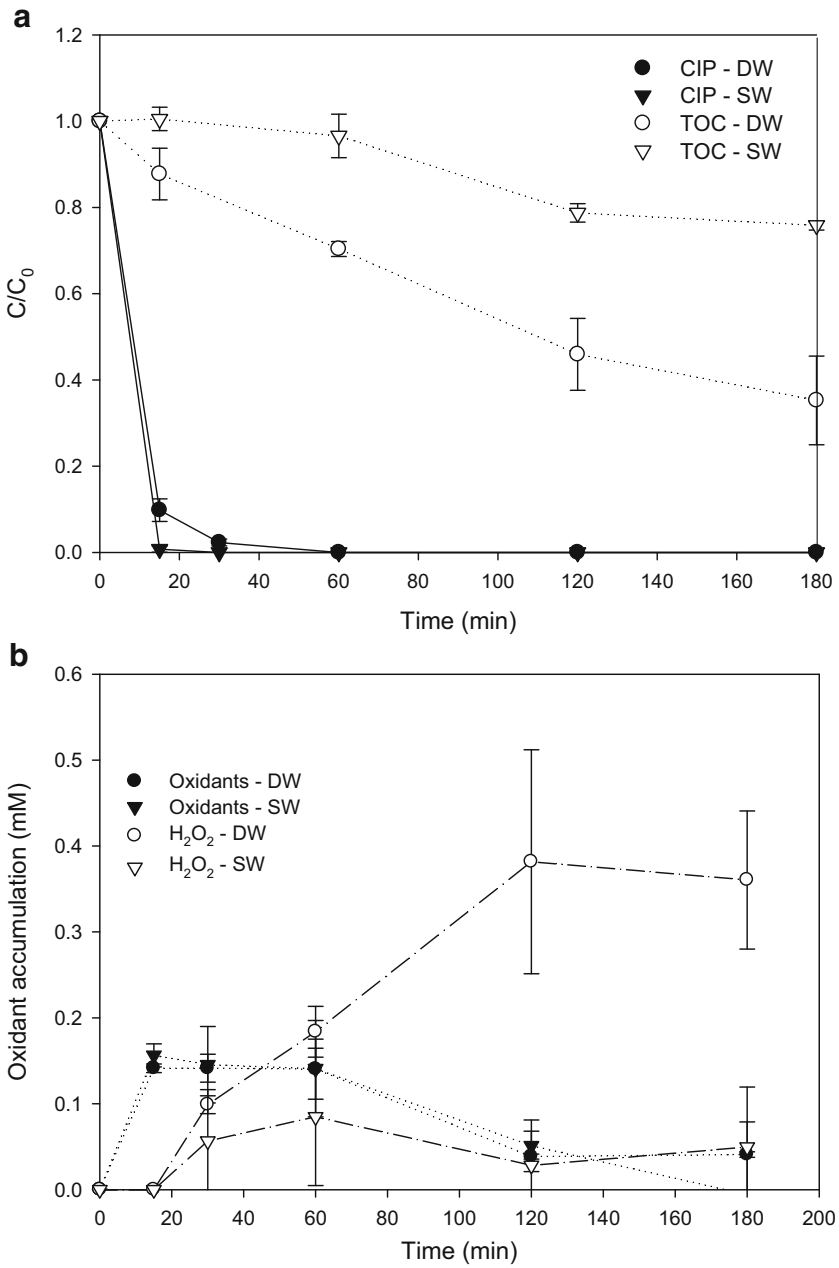

Fig. 5 **a** CIP and TOC evolution and AA elimination in distilled water (DW) and seawater (SW) during the treatment by PEF. **b** H_2O_2 evolution and other oxidant accumulation in DW and SW during PEF treatment. [CIP] = 0.1 mM; $[Fe^{2+}]$ = 0.09 mM; i = 20 mA; air flow = 840 mL min^{-1}; reactor flow = 34 mL min^{-1}

1-cyclopropyl-2,6-dihydroxy-4-oxo-7-(piperazin-1-yl)-1,4-dihydroquinoline-3-carboxylic acid; and P6, 8-chloro-1-cyclopropyl-6-fluoro-4-oxo-7-(piperazin-1-yl)-1,4-dihydroquinoline-3-carboxylic acid.

Interestingly, the results indicated that P1, P2, and P5 can be produced from UV action by itself. P1, which arises from the substitution of the F-atom by an OH group, has been reported as the main by-product of CIP photolysis (Vasconcelos et al. 2009; Paul et al. 2010; Razuc et al. 2013; Batchu et al. 2014; Haddad and Kümmerer 2014; Porras et al. 2016). The process seems to occur via an addition-elimination mechanism (SN2) [49]. P1 was also detected via HO• radical attack on CIP (Fig. 6). P5, which corresponds to the di-hydroxylated product, has also been recently reported as a photolytic CIP by-product (Batchu et al. 2014; Haddad and Kümmerer 2014; Porras et al. 2016). Meanwhile, P2, which is a product of the cleavage of the piperazine ring followed by a reductive defluorination, was also recently found during CIP photodegradation (Vasconcelos et al. 2009; Razuc et al. 2013; Haddad and Kümmerer 2014). The HO• radical attack also leads to the formation of P3 and P4. Both by-products come from the oxidative action of the HO• radical on the piperazine ring (Kugelmann et al. 2011). On the other hand, nitrogen atoms are very susceptible to chlorinated oxidative species attack (Deborde and von Gunten 2008; Giraldo et al. 2015). Therefore, an oxidative action of HOCl in the piperazine ring

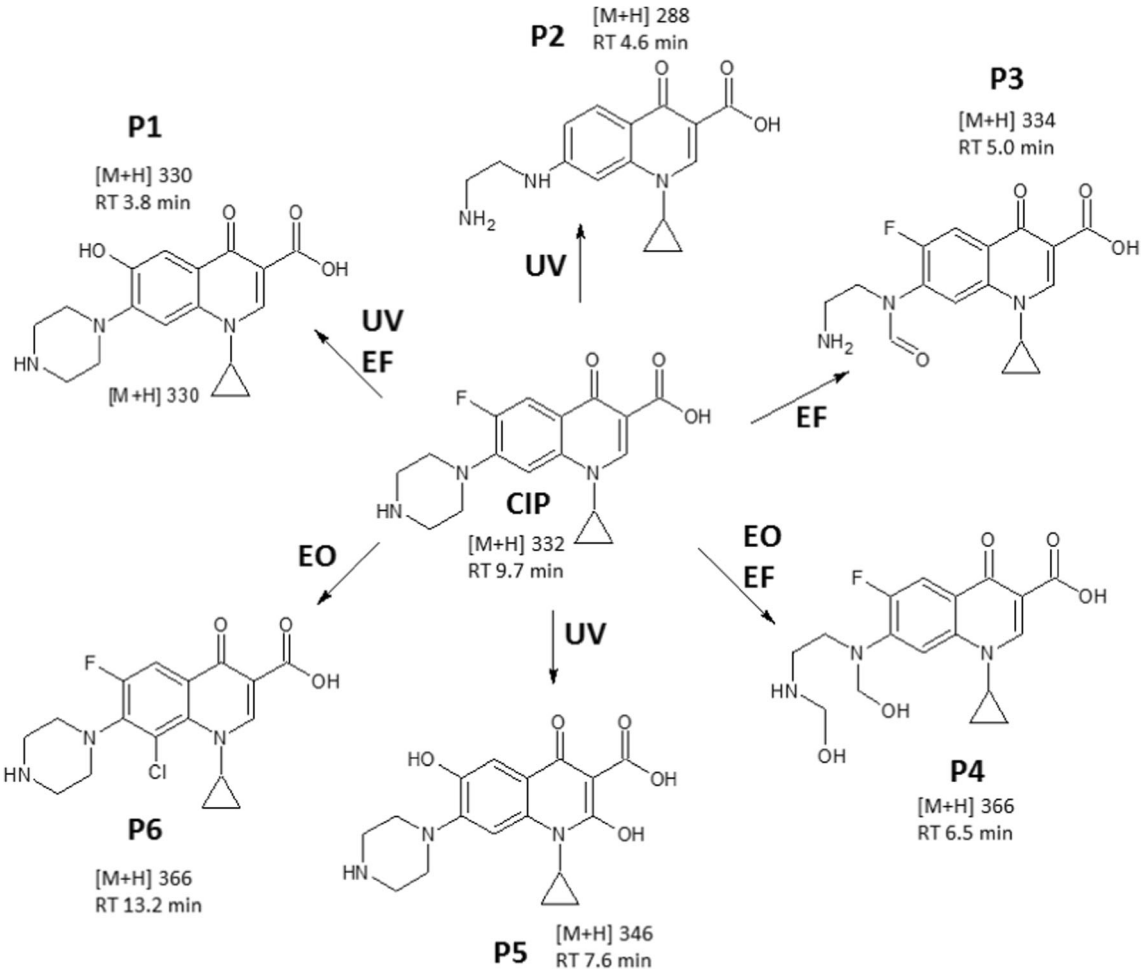

Fig. 6 CIP main by-products identified during CIP degradation when submitted to UV, EO, and EF. [CIP] = 0.1 mM; [Fe^{2+}] = 0.09 mM; i = 20 mA; air flow = 840 mL min^{-1}; reactor flow = 34 mL min^{-1}

allows the production of P4. Additionally, the electrophilic substitution of HOCl on the free ortho position on the piperazine ring leads to the by-product P6, which was also found by Dodd et al. (2005) during the oxidation of fluoroquinolones by aqueous chlorine (Dodd et al. 2005).

The chemical structure of the reported primary by-products is quite similar to the CIP molecule. Moreover, total mineralization was not reached with any process in the presence of the tested inorganic ions. Consequently, the evaluation of the antimicrobial activity (AA) of the treated solutions needs to be investigated in order to verify that the recalcitrant by-products of the PEF process do not contribute to the proliferation of the resistant bacteria. Therefore, the AA evolution during the combination of the UV, EO, and EF systems defined as PEF was determined against both a Gram-negative bacteria (*E. coli*) and a Gram-positive bacteria (*S. aureus*) (Fig. 7). Because of the higher environmental risk due to the possible formation of chlorinated organic by-products, chloride ions were selected as supporting electrolyte. The results show that only P1, P2, and P3 were identified during PEF action, suggesting that the successive attack of the species involved, especially the hydroxyl radical, easily removed P4, P5, and P6. Figure 7 also shows that the accumulation of P1 and P2 is maximized after 20 min of treatment, while P3 reaches its

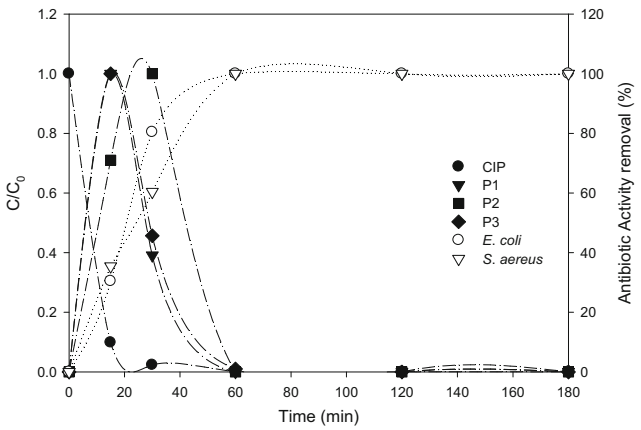

Fig. 7 CIP and main by-products evolution when submitted to PEF in the presence of chlorine and their relationship with the antibiotic activity. [CIP] = 0.1 mM; [Fe^{2+}] = 0.09 mM; i = 20 mA; air flow = 840 mL min^{-1}; reactor flow = 34 mL min^{-1}

maximum at 30 min. However, in the case of AA elimination, after 30 min significant antimicrobial activity persisted in the solution (~ 40% for *S. aureus* and ~ 20% for *E. coli*). Considering that CIP is practically eliminated after 20 min of treatment, the remaining AA could be attributed to the by-products P1, P2, and P3. This hypothesis is supported by the fact that after 40 min of treatment, when all of these by-products (P1, P2, and P3) were eliminated from the solution, antibiotic activity against both of the tested bacteria has completely stopped.

Conclusions

This investigation showed the high efficiency of the PEF system at natural initial pH as an alternative treatment of water contaminated with fluoroquinolone antibiotics such as ciprofloxacin, which contain sulfate, nitrate, and chloride anions. The effectiveness of the process can be attributed to the synergistic action of light irradiation, electro-chemical oxidation, and the Fenton reaction that degrades the pollutant in the presence of the above indicated inorganic anions, commonly known as inhibitors of the degradation of organic pollutants in advanced oxidation processes. The identification of PEF as a combination of EO, EF, and UV_{254} action allowed for the determination of several degradation pathways in which different species participate in CIP degradation depending on the inorganic ions present in the water. Direct oxidation of CIP on the anode surface was evidenced in the presence of sulfate. This also occurred in all tested PEF conditions. On the other hand, both chlorine and nitrate ions significantly improved the antibiotic elimination through the formation of secondary oxidative species. The chlorinated species were obtained by the oxidation of Cl^- at the anode (IrO_2), while the nitrogen-based oxidants were produced by the reduction of NO_3^- at the cathode (GDE). Despite the fact that the subprocesses tested (UV_{254}, EO, and EF) are able to reach total CIP elimination in many cases, only the combined PEF system, through several degradation pathways, was able to promote high levels of mineralization independently of the inorganic ion present in the solution. The involvement of different degradation pathways leads to several structural transformations of the pollutant. Therefore, six primary CIP by-products were identified (P1–P6), and the pathways generating them were determined. Direct photolysis led to the formation of P1, P2, and P5; EO led to P4 and P6; and EF produced P1, P3, and P4. Fairly similar structures were observed among the primary by-products and the antibiotic. Finally, antimicrobial activity was measured, and found to be completely removed after 60 min of PEF treatment, i.e., when CIP and the primary by-products were also eliminated. As such, it can be concluded that the antibiotics and their associated by-products can be effectively eliminated by the PEF system, and that even if HO• is mainly responsible for the CIP mineralization, IrO_3 (direct EO), HOCl, and N_{oxi} can also participate in the process, depending on the type and concentration of anions in solution. The identification of different contributions of the anions leads to the possibility of PEF being used in complex matrices such as seawater in which a mixture of anions can be found. However, in this type of water, the positive action of the anions can be suppressed by a high concentration of them in the matrix making scavenger reactions that negatively affect the system predominant.

Acknowledgements The authors would like to thank the Swiss Agency for Development and Cooperation (SDC) and the Swiss National Science Foundation (SNSF) through the project "Treatment of the hospital wastewaters in Cote d'Ivoire and in Colombia by advanced oxidation processes", the "Sostenibilidad" program of the Universidad de Antioquia, and Colciencias (Colombia) for the project "Desarrollo y evaluación de un sistema electroquímico asistido con luz solar para la eliminación de contaminantes emergentes en aguas (111565842980)".

Abbreviations *CIP*, Ciprofloxacin; *ECs*, Emergent contaminants; *DSA*, Dimensionally stable anode; *EF*, Electro-Fenton; *EO*, Electro-oxidation; *GDE*, Gas diffusional electrode; *PEF*, Photoelectro-Fentonp; *TOC*, Total organic carbon; *UV*, Ultraviolet radiation.

References

Antonin VS, Santos MC, Garcia-Segura S, Brillas E (2015) Electrochemical incineration of the antibiotic ciprofloxacin in sulfate medium and synthetic urine matrix. Water Res 83:31–41. https://doi.org/10.1016/j.watres.2015.05.066

Aquino Neto S, de Andrade AR (2009) Electrooxidation of glyphosate herbicide at different DSA® compositions: pH, concentration and supporting electrolyte effect. Electrochim Acta 54:2039–2045. https://doi.org/10.1016/j.electacta.2008.07.019

Aquino JM, Rodrigo MA, Rocha-Filho RC et al (2012) Influence of the supporting electrolyte on the electrolyses of dyes with conductive-diamond anodes. Chem Eng J 184:221–227. https://doi.org/10.1016/j.cej.2012.01.044

Babić S, Periša M, Škorić I (2013) Photolytic degradation of norfloxacin, enrofloxacin and ciprofloxacin in various aqueous media. Chemosphere 91:1635–1642. https://doi.org/10.1016/j.chemosphere.2012.12.072

Bañuelos JA, El-Ghenymy A, Rodríguez FJ et al (2014) Study of an air diffusion activated carbon packed electrode for an electro-Fenton wastewater treatment. Electrochim Acta 140:412–418. https://doi.org/10.1016/j.electacta.2014.05.078

Batchu SR, Panditi VR, O'Shea KE, Gardinali PR (2014) Photodegradation of antibiotics under simulated solar radiation: implications for their environmental fate. Sci Total Environ 470-471:299–310. https://doi.org/10.1016/j.scitotenv.2013.09.057

Bouzek K, Paidar M, Sad'ilková A, Bergmann H (2001) Electrochemical reduction of nitrate in weakly alkaline solutions. J Appl Electrochem 31:1185–1193. doi: https://doi.org/10.1023/A:1012755222981

Brillas E, Sirés I, M a O (2009) Electro-Fenton process and related electrochemical technologies based on Fenton's reaction chemistry. Chem Rev 109:6570–6631. https://doi.org/10.1021/cr900136g

Carvalho C, Fernandes a L a et al (2007) Electrochemical degradation applied to the metabolites of Acid Orange 7 anaerobic biotreatment. Chemosphere 67:1316–1324. https://doi.org/10.1016/j.chemosphere.2006.10.062

Comninellis C (1994) Electrocatalysis in the electrochemical conversion/combustion of organic pollutants for waste water treatment. Electrochim Acta 39:1857–1862. https://doi.org/10.1016/0013-4686(94)85175-1

Coria G, Sirés I, Brillas E, Nava JL (2016) Influence of the anode material on the degradation of naproxen by Fenton-based electrochemical processes. Chem Eng J 304:817–825. doi: https://doi.org/10.1016/j.cej.2016.07.012

Couto AB, Oishi SS, Ferreira NG (2016) Enhancement of nitrate electroreduction using BDD anode and metal modified carbon fiber cathode. J Ind Eng Chem 39:210–217. https://doi.org/10.1016/j.jiec.2016.05.028

Daneshvar N, Aber S, Vatanpour V, Rasoulifard MH (2008) Electro-Fenton treatment of dye solution containing Orange II: influence of operational parameters. J Electroanal Chem 615:165–174. https://doi.org/10.1016/j.jelechem.2007.12.005

De Bel E, Dewulf J, Witte BD et al (2009) Influence of pH on the sonolysis of ciprofloxacin: biodegradability, ecotoxicity and antibiotic activity of its degradation products. Chemosphere 77:291–295. https://doi.org/10.1016/j.chemosphere.2009.07.033

Deborde M, von Gunten U (2008) Reactions of chlorine with inorganic and organic compounds during water treatment—kinetics and mechanisms: a critical review. Water Res 42:13–51. https://doi.org/10.1016/j.watres.2007.07.025

Devi LG, Munikrishnappa C, Nagaraj B, Rajashekhar KE (2013) Effect of chloride and sulfate ions on the advanced photo Fenton and modified photo Fenton degradation process of Alizarin Red S. J Mol Catal A Chem 374-375:125–131. https://doi.org/10.1016/j.molcata.2013.03.023

Dima GE, De Vooys ACA, Koper MTM (2003) Electrocatalytic reduction of nitrate at low concentration on coinage and transition-metal electrodes in acid solutions. J Electroanal Chem 554-555:15–23. https://doi.org/10.1016/S0022-0728(02)01443-2

Dodd MC, Shah AD, Von Gunten U, Huang CH (2005) Interactions of fluoroquinolone antibacterial agents with aqueous chlorine: reaction kinetics, mechanisms, and transformation pathways. Environ Sci Technol 39:7065–7076. https://doi.org/10.1021/es050054e

Espinoza C, Romero J, Villegas L, et al (2016) Mineralization of the textile dye acid yellow 42 by solar photoelectro-Fenton in a lab-pilot plant. J Hazard Mater 319:24–33. https://doi.org/10.1016/j.jhazmat.2016.03.003

Feng Y, Smith DW, Bolton JR (2007) Photolysis of aqueous free chlorine species (HOCl and OCl^-) with 254 nm ultraviolet light. J Environ Eng Sci 6:277–284. https://doi.org/10.1139/s06-052

Gatica J, Cytryn E (2013) Impact of treated wastewater irrigation on antibiotic resistance in the soil microbiome. Environ Sci Pollut Res 20:3529–3538. https://doi.org/10.1007/s11356-013-1505-4

Giraldo AL, Erazo-Erazo ED, Florez-Acosta OA et al (2015) Degradation of the antibiotic oxacillin in water by anodic oxidation with Ti/IrO2 anodes: evaluation of degradation routes, organic by-products and effects of water matrix components. Chem Eng J 279:103–114. https://doi.org/10.1016/jcej2015.04.140

Grebel JE, Pignatello JJ, W a M (2010) Effect of halide ions and carbonates on organic contaminant degradation by hydroxyl radical-based advanced oxidation processes in saline waters. Environ Sci Technol 44:6822–6828. https://doi.org/10.1021/es1010225

Guo H-G, Gao N-Y, Chu W-H et al (2013) Photochemical degradation of ciprofloxacin in UV and UV/H2O2 process: kinetics, parameters, and products. Environ Sci Pollut Res 20:3202–3213. https://doi.org/10.1007/s11356-012-1229-x

Guzman-Duque F, Pétrier C, Pulgarin C et al (2011) Effects of sonochemical parameters and inorganic ions during the sonochemical degradation of crystal violet in water. Ultrason Sonochem 18:440–446. https://doi.org/10.1016/j.ultsonch.2010.07.019

Guzmán-Duque FL, Palma-Goyes RE, González I et al (2014) Relationship between anode material, supporting electrolyte and current density during electrochemical degradation of organic compounds in water. J Hazard Mater 278:221–226. https://doi.org/10.1016/j.jhazmat.2014.05.076

Haddad T, Kümmerer K (2014) Characterization of photo-transformation products of the antibiotic drug ciprofloxacin with liquid chromatography-tandem mass spectrometry in combination with accurate mass determination using an LTQ-Orbitrap. Chemosphere 115:40–46. https://doi.org/10.1016/j.chemosphere.2014.02.013

Hu S, Zhang C, Yao H et al (2015) Intensify chemical reduction to remove nitrate from groundwater via internal microelectrolysis existing in nano-zero valent iron/granular activated carbon composite. Desalin Water Treat 57:14158–14168. https://doi.org/10.1080/19443994.2015.1062430

Klamerth N, Malato S, Agüera a, Fernández-Alba A (2013) Photo-Fenton and modified photo-Fenton at neutral pH for the treatment of emerging contaminants in wastewater treatment plant effluents: a comparison. Water Res 47:833–840. https://doi.org/10.1016/j.watres.2012.11.008

Kugelmann E, Albert CR, Bringmann G, Holzgrabe U (2011) Fenton's oxidation: a tool for the investigation of potential drug metabolites. J Pharm Biomed Anal 54:1047–1058. https://doi.org/10.1016/j.jpba.2010.12.016

Lacasa E, Cañizares P, Llanos J, Rodrigo MA (2011) Removal of nitrates by electrolysis in non-chloride media: effect of the anode material. Sep Purif Technol 80:592–599. https://doi.org/10.1016/j.seppur.2011.06.01510.1016

Lacasa E, Cañizares P, Llanos J, Rodrigo MA (2012) Effect of the cathode material on the removal of nitrates by electrolysis in non-chloride media. J Hazard Mater 213-214:478–484. https://doi.org/10.1016/j.jhazmat.2012.02.034

Lacasa E, Tsolaki E, Sbokou Z et al (2013) Electrochemical disinfection of simulated ballast water on conductive diamond electrodes. Chem Eng J 223:516–523. https://doi.org/10.1016/j.cej.2013.03.003

Liang J, Zheng Y, Liu Z (2016) Nanowire-based Cu electrode as electrochemical sensor for detection of nitrate in water. Sensors Actuators B Chem 232:336–344. https://doi.org/10.1016/j.snb.2016.03.145

Luo H, Li C, Wu C et al (2015) Electrochemical degradation of phenol by in situ electro-generated and electro-activated hydrogen peroxide using an improved gas diffusion cathode. Electrochim Acta 186:486–493. https://doi.org/10.1016/j.electacta.2015.10.194

Malpass GRP, Miwa DW, Miwa ACP et al (2007) Photo-assisted electrochemical oxidation of atrazine on a commercial Ti/Ru0.3Ti0.7O2 DSA electrode. Environ Sci Technol 41:7120–7125. https://doi.org/10.1021/es070798n

Martínez-Huitle CA, Brillas E (2009) Decontamination of wastewaters containing synthetic organic dyes by electrochemical methods: a general review. Appl Catal B Environ 87:105–145. https://doi.org/10.1016/j.apcatb.2008.09.017

Nogueira RFP, Oliveira MC, Paterlini WC (2005) Simple and fast spectrophotometric determination of H(2)O(2) in photo-Fenton reactions using metavanadate. Talanta 66:86–91. https://doi.org/10.1016/j.talanta.2004.10.001

Palma-Goyes RE, Guzmán-Duque FL, Peñuela G et al (2010) Electrochemical degradation of crystal violet with BDD electrodes: effect of electrochemical parameters and identification of organic by-products. Chemosphere 81:26–32. https://doi.org/10.1016/j.chemosphere.2010.07.020

Panizza M, Martinez-Huitle CA (2013) Role of electrode materials for the anodic oxidation of a real landfill leachate—comparison between Ti–Ru–Sn ternary oxide, PbO2 and boron-doped diamond anode. Chemosphere 90:1455–1460. https://doi.org/10.1016/j.chemosphere.2012.09.006

Paul T, Dodd MC, Strathmann TJ (2010) Photolytic and photocatalytic decomposition of aqueous ciprofloxacin: transformation products and residual antibacterial activity. Water Res 44:3121–3132. https://doi.org/10.1016/j.watres.2010.03.002

Pérez T, Sirés I, Brillas E, Nava JL (2017) Solar photoelectro-Fenton flow plant modeling for the degradation of the antibiotic erythromycin in sulfate medium. Electrochim Acta. 228:45–56. https://doi.org/10.1016/j.electacta.2017.01.047

Pignatello JJ, Oliveros E, MacKay A (2006) Advanced oxidation processes for organic contaminant destruction based on the Fenton reaction and related chemistry. Crit Rev Environ Sci Technol 36:1–84. https://doi.org/10.1080/10643380500326564

Porras J, Bedoya C, Silva-Agredo J et al (2016) Role of humic substances in the degradation pathways and residual antibacterial activity during the photodecomposition of the antibiotic ciprofloxacin in water. Water Res 94:1–9. https://doi.org/10.1016/j.actamat.2015.02.029

Razuc M, Garrido M, Caro YS et al (2013) Hybrid hard- and soft-modeling of spectrophotometric data for monitoring of ciprofloxacin and its main photodegradation products at different pH values. Spectrochim Acta - Part A Mol Biomol Spectrosc 106:146–154. https://doi.org/10.1016/j.saa.2012.12.085

Rubio-Clemente A, Torres-Palma RA, Peñuela GA (2014) Removal of polycyclic aromatic hydrocarbons in aqueous environment by chemical treatments: a review. Sci Total Environ 478:201–225. https://doi.org/10.1016/j.scitotenv.2013.12.126

Rudolf M, Roušar I, Krýsa J (1995) Influence of ion migration on cathodic reduction of hypochlorite anions. Electrochim Acta 40:169–174. https://doi.org/10.1016/0013-4686(94)00310-W

Sánchez-Carretero A, Sáez C, Cañizares P, Rodrigo MA (2011) Electrochemical production of perchlorates using conductive diamond electrolyses. Chem Eng J 166:710–714. https://doi.org/10.1016/j.cej.2010.11.037

Serna-Galvis EA, Silva-Agredo J, Giraldo AL et al (2016) Comparative study of the effect of pharmaceutical additives on the elimination of antibiotic activity during the treatment of oxacillin in water by the photo-Fenton, TiO2-photocatalysis and electrochemical processes. Sci Total Environ 541:1431–1438. https://doi.org/10.1016/j.scitotenv.2015.10.029

Serna-Galvis EA, Ferraro F, Silva-Agredo J, Torres-Palma RA (2017a) Degradation of highly consumed fluoroquinolones, penicillins and cephalosporins in distilled water and simulated hospital wastewater by UV254 and UV254/persulfate processes. Water Res 122:128–138. https://doi.org/10.1016/j.watres.2017.05.065

Serna-Galvis EA, Jojoa-Sierra SD, Berrio-Perlaza KE et al (2017b) Structure-reactivity relationship in the degradation of three representative fluoroquinolone antibiotics in water by electrogenerated active chlorine. Chem Eng J 315:552–561. https://doi.org/10.1016/j.cej.2017.01.062

Sirés I, Brillas E, Oturan MA et al (2014) Electrochemical advanced oxidation processes: today and tomorrow. A review. Environ Sci Pollut Res 21:8336–8367. https://doi.org/10.1007/s11356-014-2783-1

Sturini M, Speltini A, Maraschi F et al (2015) Sunlight-induced degradation of fluoroquinolones in wastewater effluent: photoproducts identification and toxicity. Chemosphere 134:313–318. https://doi.org/10.1016/j.chemosphere.2015.04.081

Thiam A, Zhou M, Brillas E, Sirés I (2014) Two-step mineralization of tartrazine solutions: study of parameters and by-products during the coupling of electrocoagulation with electrochemical advanced oxidation processes. Appl Catal B Environ 150-151:116–125. https://doi.org/10.1016/j.apcatb.2013.12.011

Torres RA, Sarria V, Torres W et al (2003) Electrochemical treatment of industrial wastewater containing 5-amino-6-methyl-2-benzimidazolone: toward an electrochemical-biological coupling. Water Res 37:3118–3124. https://doi.org/10.1016/S0043-1354(03)00179-9

Vasconcelos TG, Henriques DM, König A et al (2009) Photo-degradation of the antimicrobial ciprofloxacin at high pH: identification and biodegradability assessment of the primary by-products. Chemosphere 76:487–493. https://doi.org/10.1016/j.chemosphere.2009.03.022

Villegas-Guzman P, Silva-Agredo J, Giraldo-Aguirre AL et al (2014) Enhancement and inhibition effects of water matrices during the sonochemical degradation of the antibiotic dicloxacillin. Ultrason Sonochem 22:211–219. https://doi.org/10.1016/j.ultsonch.2014.07.006

Villegas-Guzman P, Silva-Agredo J, González-Gómez D et al (2015) Evaluation of water matrix effects, experimental parameters, and the degradation pathway during the TiO2 photocatalytical treatment of the antibiotic dicloxacillin. J Environ Sci Health A Tox Hazard Subst Environ Eng 50:40–48. https://doi.org/10.1080/10934529.2015.964606

Villegas-Guzman P, Oppenheimer-Barrot S, Silva-Agredo J, Torres-Palma RA. (2017) Comparative evaluation of photo-chemical AOPs for ciprofoxacin degradation: elimination in natural waters and analysis of pH effect, primary degradation by-products, and the relationship with the antibiotic activity. Water Air Soil Pollut 228:209–214. doi: https://doi.org/10.1007/s11270-017-3388-3

Xiao R, He Z, Diaz-Rivera D et al (2014) Sonochemical degradation of ciprofloxacin and ibuprofen in the presence of matrix organic compounds. Ultrason Sonochem 21:428–435. https://doi.org/10.1016/j.ultsonch.2013.06.012

Xu W, Zhang G, Li X et al (2007) Occurrence and elimination of antibiotics at four sewage treatment plants in the Pearl River Delta (PRD), South China. Water Res 41:4526–4534. https://doi.org/10.1016/j.watres.2007.06.023

Zhou M, Särkkä H, Sillanpää M (2011) A comparative experimental study on methyl orange degradation by electrochemical oxidation on BDD and MMO electrodes. Sep Purif Technol 78:290–297. https://doi.org/10.1016/j.seppur.2011.02.013